Histograms of the Kirchhoff migration operator

James Close and John C. Bancroft

ABSTRACT

A new method of Kirchhoff migration is examined which utilizes a histogram to isolate for amplitude coherency along each diffraction shape. A histogram of amplitude frequencies is used to eliminate non-coherent and small amplitude data from the final migration summation. The method explored is data driven as opposed to model driven, which allows the definition of a space varying migration aperture without the need for a preconceived model.

In this method, a histogram is formed of the frequency of amplitudes along each diffraction shape defined by Kirchhoff migration. It was found that if a constant amplitude scale is applied to our histogram, similar results are produced by applying an energy threshold mute to the data. It was also found that varying the histogram amplitude scale, according to the maximum energy on each diffraction shape, biased small amplitude data which aliased the migration output.

It was concluded that this method works well for eliminating noise and spikes in the data while preserving dipping events, diffraction events, and flat events, which could have practical application for examining spiky seismic data.

INTRODUCTION

In migrating seismic data, there are three main methods which are used; Kirchhoff, Fourier transform (FK), and downward continuation (for example finite difference and phase shift migration) (Bancroft, 2008). Kirchhoff migration is a widely used tool for both time and depth imaging and iterative velocity analysis. Algorithms used for Kirchhoff migration range from the very simple to the relatively complex, although the following main principles are followed in each variation: For each migrated output sample, diffraction curves (hyperbolic paths) are defined at migration output locations; the energy within that diffraction shape is then weighted and summed. The summed value is then inserted at the migrated position (being the amplitude value at the output location) and then, if desired, additional scaling and filtering can be applied. The diffraction shape for a Kirchhoff time migration is computed using equation (1), where x is the distance between the input and migrated trace, T_0 the two-way time at zero offset, and V the velocity defined at T_0 (Bancroft, 2008).

$$T^2(x) = T_0^2 + \frac{4x^2}{V^2(T_0)} \qquad (1)$$

The size of the diffraction, also known as the aperture, is usually limited by the dip angles and/or a maximum offset. In general, as the migration aperture is increased, the migration fidelity is improved. However, since seismic data sets consist of discrete trace sampling, the aperture must be restricted to avoid the degrading effects of spatial aliasing (Kosloff et al., 1997). A taper can also be applied which zeroes the data over a small

range of dips at the dip limit. The amplitude of the data is then usually weighted using equation (2) (Bancroft, 2008).

$$Amp(x) = \frac{T_0}{T} \tag{2}$$

Antialiasing is important for improving imaging in Kirchhoff migration. Aliasing may occur in the input data, the migration algorithm (operator), or the output data. Aliasing problems caused by the input data generally happen for two reasons. One reason aliasing may occur on the input data is due to coarse trace spacing which does not support events over a certain dip angle. This type of aliasing can be explained by equation (3), known as the aliasing equation, where f_m is the maximum cutoff (unaliased) frequency, CMP_x is the trace spacing, V is the velocity, and α is the dip angle. This implies that we want to choose our maximum cutoff frequency as defined in equation (4) where $\frac{\partial t}{\partial x}$ is the migration operator slope, and ΔT is the relative time shift of the operator between the two traces (Abma et al., 1999). This means that ΔT must increase with the dip for an anti-aliasing filter applied to the diffraction shape.

$$f_m = \frac{V}{4CMP_x \tan\alpha} = \frac{1}{2\Delta T} \tag{3}$$

$$f_m \leq \frac{1}{2\Delta T} = \frac{1}{2\frac{\partial t}{\partial x}CMP_x} \tag{4}$$

The second common cause of aliasing on the input data is due to sampling frequency along each trace. This is known as the Nyquist criterion, which requires the sampling frequency must be greater than twice the maximum frequency, or in other words, there to be at least two samples per cycle for the period of the highest frequency of the signal (Bancroft 2008). In data processing, compromises must be made over what sampling rate to use due to the resulting high memory requirements and longer run times caused by higher sampling rates.

Even if we have perfect input data in which no aliasing occurs, we can still get aliased migration data due to our operator, or migration algorithm. Since basic Kirchhoff migration passes a diffraction shape over our input data without taking the frequency content of the data into consideration we can get operator aliasing. For example, the steep part of a diffraction shape may under-sample the seismic wavelet as it passes over a flat portion of the un-migrated data. One way to overcome this problem is to reduce the frequency content of the data encountered by the steep part of the diffraction shape (Gray et al., 2001).

In the 2D zero-offset constant-velocity case of Kirchhoff migration, the number of output data points is normally defined as equal to the number of input data samples which is also equal to the number of diffraction summations that we perform over our data set. If we decide that this number of output samples is not optimal, then we can choose a different output trace and sample spacing. Since it is difficult to determine a perfect solution for output trace and sample spacing, we can assume at least a small amount of output data aliasing.

As previously mentioned, in order to apply a proper migration to our seismic data, an aperture must be defined as large enough to properly migrate dipping data and yet not so large as to introduce artifacts from spatial aliasing. Once an aperture is defined for a given data set, the aperture normally remains constant throughout the entire migration process (Kosloff et al., 1997). Since the characteristics of a data set can have drastic variation, an aperture selected for one part of the data section may not be optimum for another part. In order to address this problem, Kosloff et al. (1997) propose a method of migration which uses a model-based aperture technique in order to determine the range of the seismic data that is most relevant for imaging a selected area in depth.

The model-based migration method automatically calculates a migration aperture size from a seismic data set to be migrated, rather than rely on user judgment to determine the aperture size (note that this migration aperture is space varying). It uses a different migration aperture for every part of the seismic data and also limits the area to be migrated as defined by a displacement section of the data (Kosloff et al., 1997). The result is that only imaged points within the local aperture are considered for the summation value of the migration output, that is, if we picture this as a basic Kirchhoff migration diffraction shape, only a select amount of the data over the diffraction (the coherent energy) will be added to our migration value (as opposed to summing over the entire diffraction).

Although this model-based migration method addresses the problem caused by having a constant aperture, it introduces a brand new problem - the requirement of a preconceived model. That is, it requires the formation of a velocity section and a depth model from the CMP gathers, and then forms a displacement model (used to calculate the space dependent aperture) by ray tracing the velocity section and the depth model. Therefore if the wrong model is chosen, everything that follows will also be wrong. The resulting migration output will tend to verify the wrong model leading to interpretation errors.

This paper introduces a method which is similar to the model-based migration method of Kosloff et al. (1997) except that it is data-driven instead of model-driven, eliminating some of the problems resulting from requiring a preconceived model. In our method, we use a histogram of the amplitudes for each diffraction shape in Kirchhoff migration in order to isolate for the coherent energy along that diffraction. This essentially forms a different aperture for every migration location with the aperture being defined by the input data. This can minimize interpretation errors since the results will be based strictly on the seismic data and not on any preconceived model of the subsurface.

INPUT MODEL

A numerical input model called Mod50 (Figure 1) was used to perform our migration and test our method. This model has a constant velocity of 10000 ft/sec. It contains linear and dipping reflections, diffractions, and localized points of reflection energy. The model has 150 traces with a trace interval of 100 ft. It is sampled at a 2 ms sample rate for a total time of 1.5 seconds resulting in a total of 750 time samples for each trace. After defining all the events, the entire section was bandpass filtered to a maximum

frequency of 50 Hz. We use a constant velocity over the entire model in order to migrate our results (Bancroft, 2008).

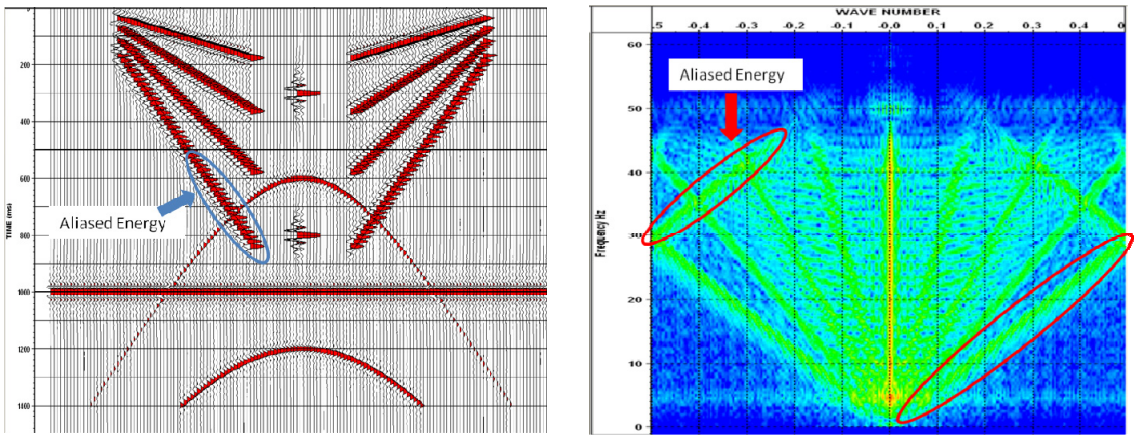

a) b)

FIG. 1 Input model and its FK transform

If we examine the FK transform of Mod50, we can see that the energy is band limited to 50 Hz. We can also see the aliased energy from the two steeper dipping events that have wrapped around (inside blue circle on Figure 1a and red circle on Figure 1b) (Bancroft, 2008). This aliased energy occurs due to the Nyquist criterion – for example, we can see that there is a distinct separation between the wavelets at the bottom of our steepest dipping event (circled in blue in Figure 1) whereas there is little separation occurring for the three shallower dipping events.

HISTOGRAM MIGRATION ALGORITHM – THEORY AND EXAMPLES

The algorithm to perform our histogram migration method was written in FORTRAN and built upon John Bancroft's (1993) basic Kirchhoff migration code. It consists of the following seven distinct steps, each of which will be discussed in detail, including examples from our input model (Section 3). Note that any desired filtering to the input data (such as a rho filter) may be implemented prior to performing the histogram migration.

1. A diffraction shape (defined, in our case, by an angle aperture with a taper) is constructed for each data sample over each trace (as in basic Kirchhoff migration) defining an amplitude array.
2. Amplitude scaling and smoothing is applied to the amplitude array.
3. A fixed-scale histogram of amplitudes is constructed for each array.
4. Noise, defined as small amplitude energy, is removed from the histogram.
5. The histogram is smoothed (we use a box-car filter).
6. The amplitude coherency of highest frequency within the histogram is isolated.
7. The migration output energy is calculated using the coherent energy isolated from the histogram.

1 Diffraction Shape

After any desired initial filtering is applied to the input data (for example, a rho filter), the algorithm loops through the desired migration output locations. In this case we chose the simple method of looping over every sample for every trace. All seven steps are performed on each sample (migration output location) before moving on to the next. For each sample a diffraction shape is computed using equation (1). A dip limited (angle) migration aperture and a diffraction taper were also included as per the basic Kirchhoff migration method.

In order to provide a visual example of what is happening, we will focus on two data points which occur at the same locations on our input model and our migration due to our choice of having every data sample represent a migration output location.

The two points which we will examine are defined as Point 1 – located at trace 20, sample 135, and Point 2 – located at trace 55, sample 125. These two points represent migrated data on (Figures 3 and 4) and off (Figures 5 and 6) a reflector. We will show the difference between the energy that is isolated at these points using our histogram method.

Figure 2a shows a diffraction shape (illustrated, not the true diffraction) which is tangential to our steepest dipping event (Location A) and also passes through our horizontal event (B) and our deepest diffraction event (C). Circled in black is the energy that we want to isolate for and migrate to our Point 1 location indicated in Figure 2b. The migration in Figure 2b shows a basic Kirchhoff migration where the output energy was summed over the entire diffraction, which in this case is inclusive of all the energy from A, B, C, and any other small noise or events along the diffraction.

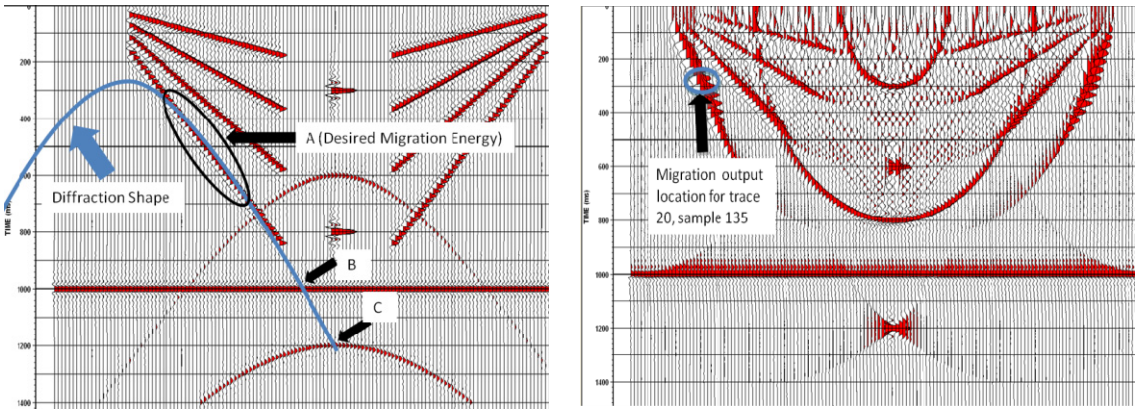

a) b)

FIG. 2 A diffraction tangent to a reflector in a) places the energy at the apex of the diffraction as highlighted in b) at trace 20 and time 170 ms.

Examining Figure 3a, we see that our diffraction shape now passes through many events (labeled A to G) but is not actually tangential to any events (note that this is not the true diffraction shape, but an illustration showing the approximate locations). Since it is not tangential to any of our events, it will not represent any real events in our migration. We can see this in Figure 3b where there is aliasing (noise) at our output

location. Instead of wanting to keep coherent energy as part of the migration, as was previously desired for Point 1, we now want to eliminate all energy along this diffraction. The remaining steps will show how the histogram method aims to accomplish this.

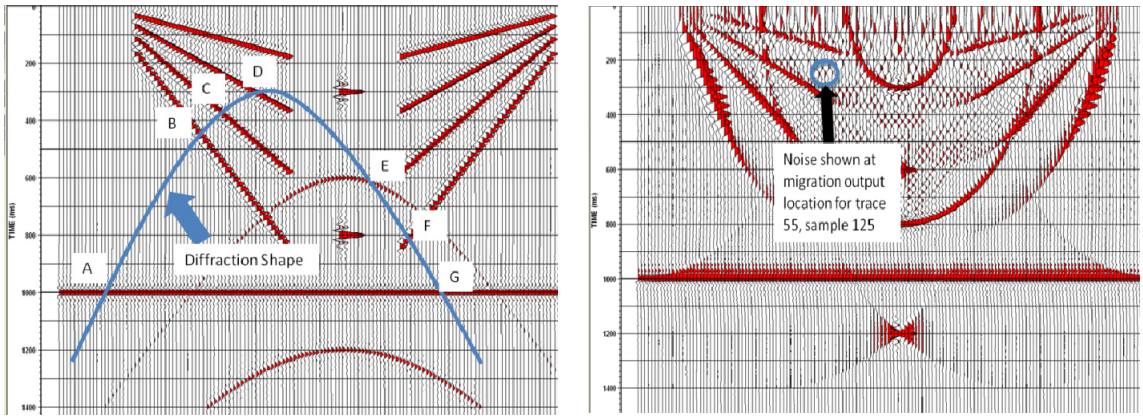

a) b)

FIG. 3 Diffraction shape located in a) over non-tangential events and in b) the aliasing noise.

2 Construct Array of Diffraction Amplitudes

Once a diffraction shape has been defined, we construct an array of amplitudes representing the amplitude of the energy at every point on the diffraction. This amplitude array can be scaled, smoothed, or have any other filter applied to it if desired. We chose to smooth the data using a 3-point boxcar filter.

Figures 4a and (b) show the amplitudes along our diffraction shapes at Point 1 and Point 2 (respectively) prior to smoothing. Examining Figure 4a, we can see the amplitude representing the portion of our diffraction shape which is tangential to the steepest dipping event in our model (location A, circled in red). The spike of high amplitude at point B occurs due to the diffraction passing through our horizontal event and the small spike of amplitude at point C represents when the migration diffraction passes through the deepest diffraction event of our input model.

Examining Figure 4b, we see seven distinct spikes of positive amplitude which are lettered corresponding to when they occur on our input model (Figure 2b). The spikes at A and G represent the two occurrences of our diffraction passing through the horizontal event. The spikes at B through D represent when the diffraction passes through our three dipping events to the left of our model, spike E occurs when the diffraction passes through the shallowest diffraction event, and finally spike F represents when the diffraction just catches the bottom of our steepest dipping event on the right of our model. Our goal is to eliminate the energy of all of these spikes in Figure 4b as this energy is only representative of noise and not of any real events. The first step towards eliminating these energy spikes is to apply amplitude smoothing.

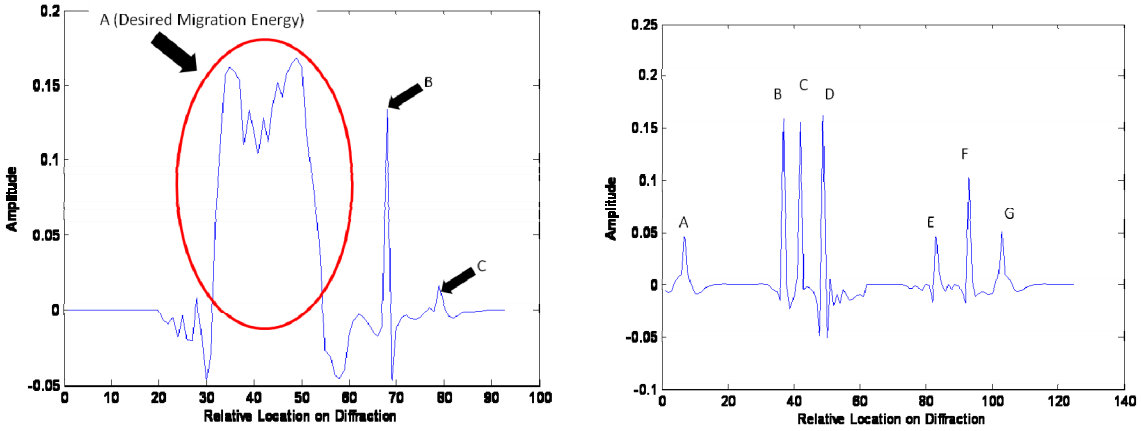

a) b)

FIG. 4 Amplitudes of the energy along the diffraction shape in a) from Figure 2a and in b) from Figure 3a. The letters in these figures correspond to the locations in those figures.

Examining Figures 5a and b) we can see what happens after smoothing. A 3-point boxcar filter was applied three times (3BX3) to our amplitude arrays, and as we can see, the amplitudes of the spikes have been greatly diminished for both Point 1 and Point 2. At the same time our desired migration energy, circled in red, has remained at approximately the same high amplitude as desired.

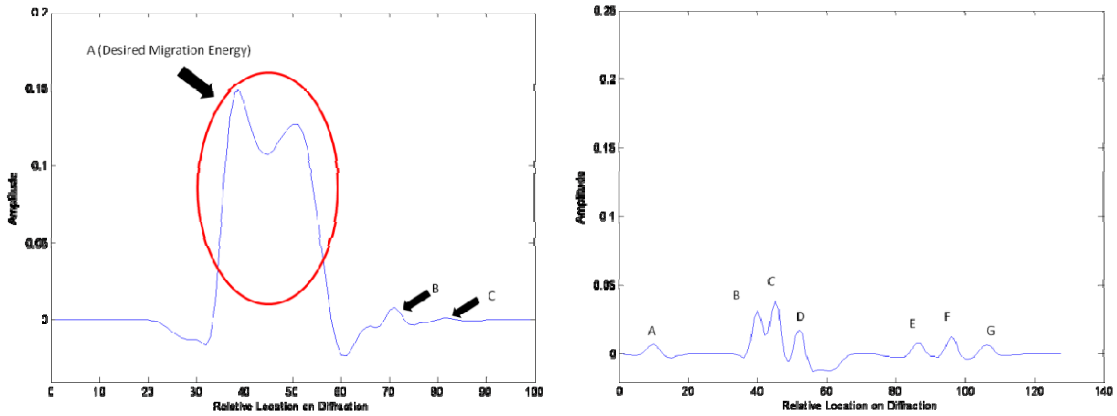

b) b)

FIG. 5 Amplitudes along the diffraction after smoothing with a 3-point boxcar 3 times.

3 Construct a Histogram of Amplitude Frequency

We now use our (smoothed) amplitude array to construct a histogram of the frequency of the amplitudes. The histogram is defined from the negative amplitude value of a user defined threshold energy to the positive amplitude value of this energy. The threshold energy must be chosen by examining the data. For our case it was found that an amplitude threshold of approximately 0.1 gave us our best results (see Section 6). For our example Points 1 and 2, we will show what happens when the amplitude threshold is chosen as approximately 0.15 as this gives a nice example of how non-coherent energy (spikes and noise) are eliminated from our migration. The histogram can be divided into any amount of bins as defined by the user, and in our example case was divided into

twenty-one equal sized bins. After the scale and bin sizes are defined, the amplitude frequencies are assigned to each of the bins.

Figures 6a and (b) show the amplitude frequencies for the diffraction shapes originating at Points 1 and 2 respectively. As expected, both histograms are dominated by zeroes and very small amplitudes which represent most of our noise. Note, however, that in some cases we may have some small amplitude or non-coherent amplitudes that represents real events, data spikes are one example of this (a buried pipe for instance). As we will see, we eliminate this energy using the histogram method, and in such cases, our method has application where the removal of spikes and the migration of larger, more energy coherent events is desired.

An important feature to notice is that in Figure 6 (for Point 2) all of the amplitudes are relatively close to zero compared to that of Figure 5b (for Point 1) where we get amplitudes higher than 0.1. This reiterates the fact that smoothing our data with the boxcar filter has already eliminated a fair amount of noise.

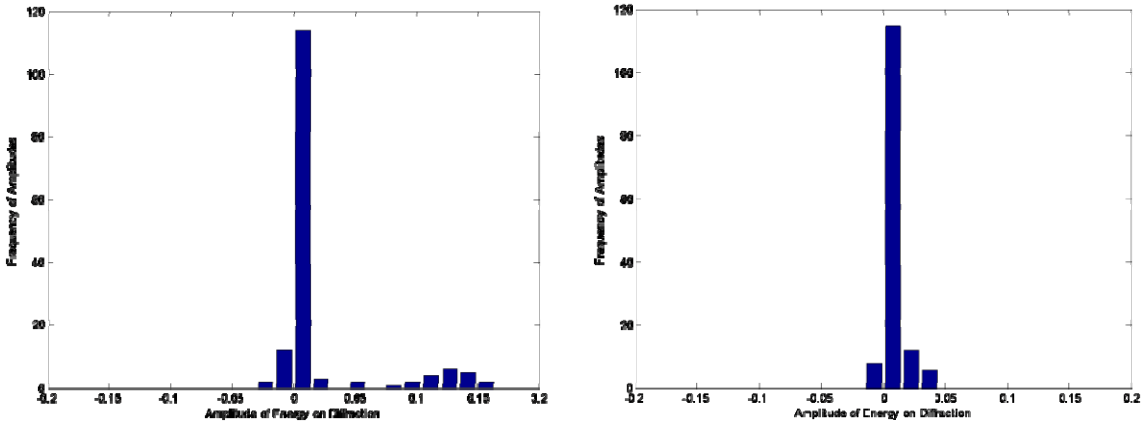

a) b)

FIG . 6 Histograms for diffraction amplitudes in a) for Point 1, and b) for point 2.

4 Removal of Noise (Small Amplitude) from Histogram

The next step in our histogram anti-aliasing method is to eliminate the small values (and zeroes) on our histograms which most likely represent noise, but also can represent real event spikes. It is a case-by-case decision based on the input data to decide what portion of bins to remove. For our input model, it was decided that the elimination of the bin representing zero amplitude along with three bins on either side of this gave optimal results.

After the small energy values are eliminated, we are either left with just the high amplitudes, which may be of high positive or high negative amplitude in Figure 7a, or we may have already eliminated all noise and spikes (non-coherent energy) in Figure 7b. Now it is simply a matter of smoothing our histogram data for the high amplitude coherent energy, which will better focus our desired migration output energy as well as further diminish any noise not caught by our filtering of the mplitudes along our diffraction and our histogram zeroing method.

Note that in the case of a histogram having both high positive and high negative amplitudes, either the positive or negative energy is chosen and extracted based on the frequency of this coherent energy in the histogram as we will later see.

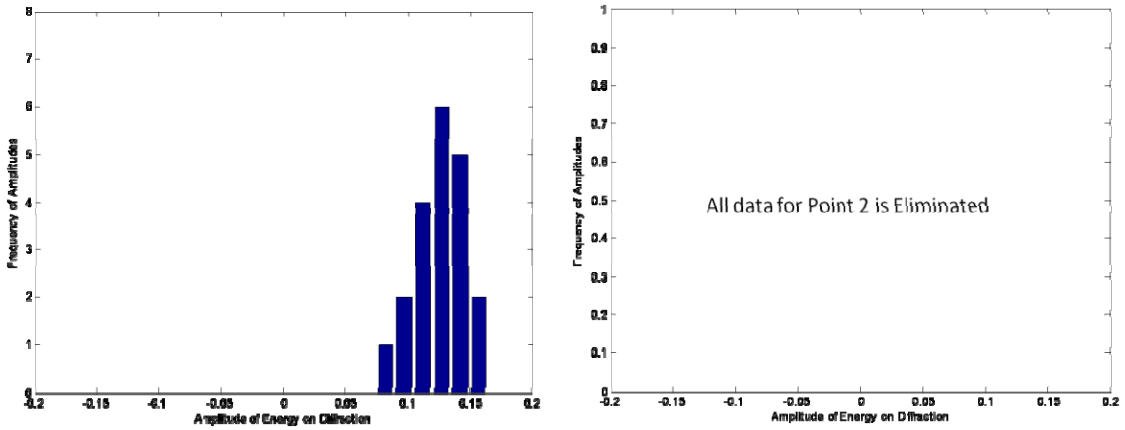

a) b)

FIG. 7 Histograms after zeroing energy.

5 Histogram Smoothing

After eliminating the small energy values from our diffraction, we smooth our histogram data. We chose to apply a 3-point boxcar filter three times just as we did to the amplitude array. We want to search for amplitude coherency, which is expected to represent real events in our data. Smoothing the amplitude frequencies over our histogram has the desired effect of focusing our data in a more coherent manner. Smoothing the histogram also has the effect of further decreasing the amplitude of single bins which may have escaped our zeroing method and represent noise.

When convolving a box-car (running average) filter together with itself many times, the central limit theorem states that the resulting shape will tend to a Gaussian. This effect could be seen previously in Figure 5 after the amplitude arrays were smoothed, and it can also be seen after boxcar smoothing was applied to the histogram.

Figures 8a is boxcar filtered once, Figure 8b boxcar filtered twice, and Figure 8c boxcar filtered three times to show the smoothing progression of the coherent high energies for the diffraction originating at Point 1. Note that since the energy for Point 2 has already been eliminated after zeroing our small amplitude histogram values, there is no need to look at the effect of smoothing the histogram on this diffraction.

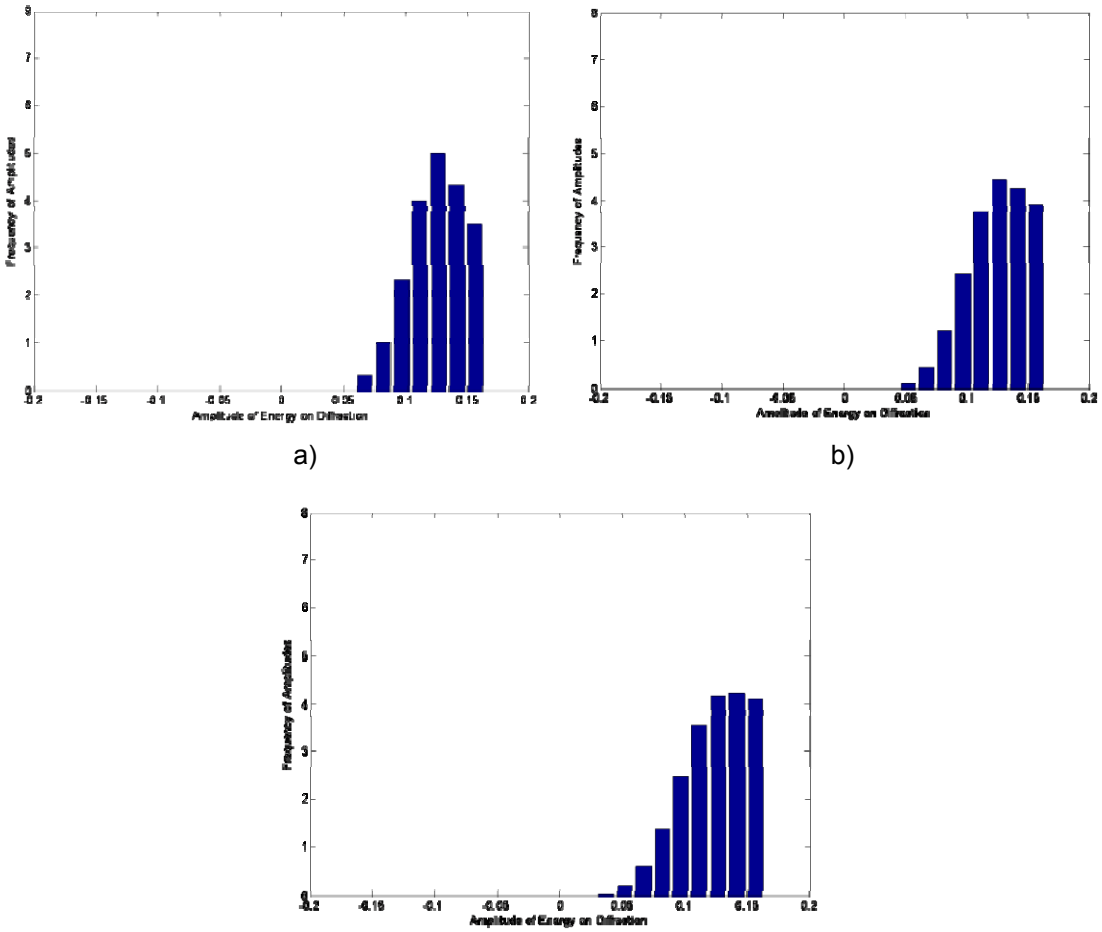

FIG. 8 Histogram energy a) for boxcar filtering once, b) boxcar filtering twice, and c) boxcar filtering three times.

6 Isolate for Highest Frequency Amplitude Coherency

As previously mentioned, it is expected that some diffractions will contain energy of both high positive and negative amplitudes representing events. In our method we simply compare the frequency of coherent negative versus positive high amplitude on the histogram and choose whichever amplitude has the highest frequency in order to use as our migration energy. Note that the fact we are potentially eliminating a large portion of high amplitude (positive or negative) could eliminate events which we would like to image, as a slight frequency advantage of positive amplitude over negative amplitude for example, may mean that a negative amplitude event, which may be desired over the positive event, is entirely eliminated.

For our example diffraction originating at Point 1, Figure 8c represents the amplitude frequency histogram which will be used to calculate our migration output energy. We have isolated for a grouping of coherent high amplitude positive energy in this case, which represents a portion of our steepest dipping event. In the case of the diffraction originating at Point 2, which we have seen represented noise, all the energy has been eliminated as desired.

7 Compute Migration Output Energy for Input Sample Location

The final output for our migration is weighted as the amplitude of the bin with the highest frequency within the coherent section of the histogram (the highest amplitude is chosen if more than one bin has the same high frequency), multiplied by this frequency, and then multiplied by the width of the coherent histogram section. This energy is then placed at the top of our diffraction which results in our migration output.

We can now make an approximate calculation of what our migration output energies will be for Points 1 (we know it is zero for Point 2). Examining Figure 8c for Point 1 which represents our real event, we can see that the bin containing the highest frequency of approximately 4.25 is located at the amplitude of approximately 0.14. The width of the coherent energy section is 9 bins; therefore for the location at Point 1 (trace 20, sample 135) we get a migration output energy of approximately 4.25*0.14*9 = 5.4.

RESULTS

We will now examine and compare various migration outputs resulting from modifications to our algorithm. We will look at the FK Spectrum for each output. For ease of comparison, Figure 9 shows our input model and Figure 10 shows the result of basic Kirchhoff migration without an aperture, taper, or any filtering.

Figure 11 shows our final migration (and FK spectrum) after a rho filter was applied to the input data, an angle aperture and diffraction taper were defined (80 degrees for aperture, 70 degrees for taper), amplitude scaling was applied to the amplitude spectrum of each diffraction, a 3-point boxcar filter was applied to the amplitude spectrum of each diffraction three times, and a 3-point boxcar filter was applied to the zeroed histogram three times. Figure 11 was given an amplitude threshold of 0.1. Note that this migration has eliminated our diffraction events as well as our spiking events.

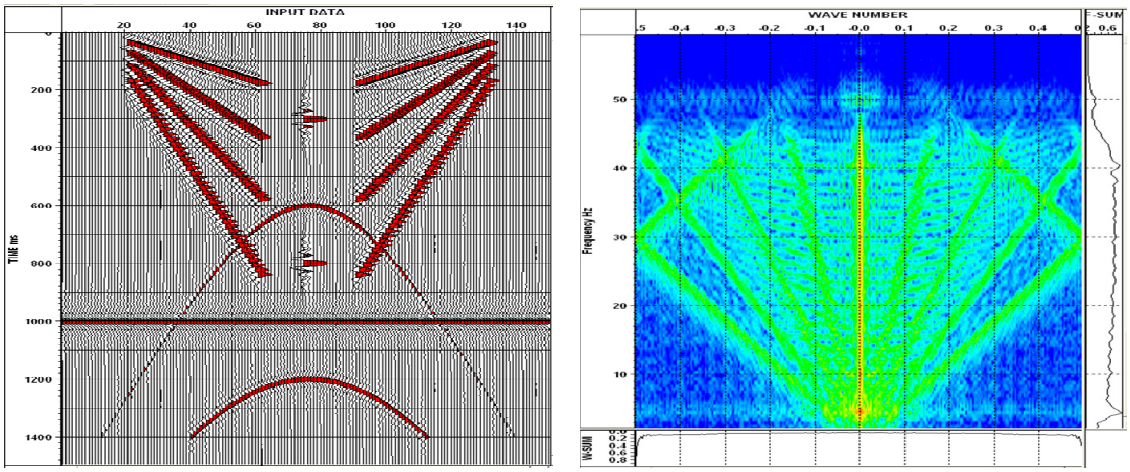

a) b)

FIG. 9 Input model a) and in b) its FK transform.

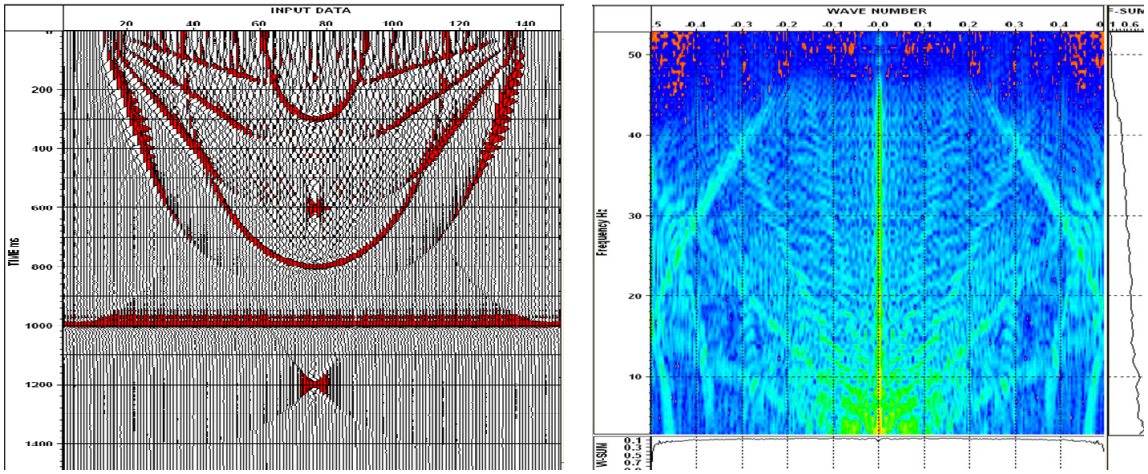

a) b)

FIG. 10 Basic Kirchhoff migration of the model in a), and in b) the FK transform.

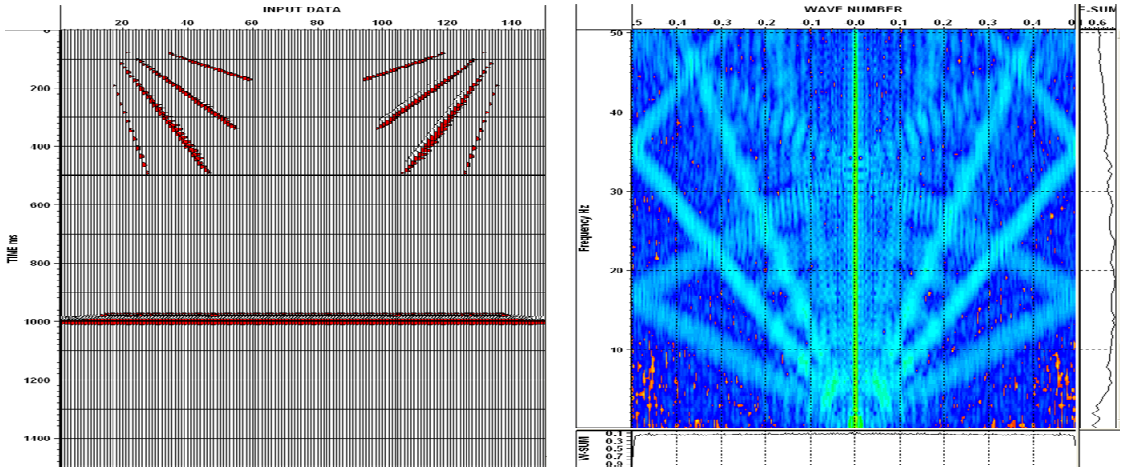

a) b)

FIG. 11 The migration in a), and the FK transform after a histogram threshold of 0.l, rho filter, aperture taper, amplitude scaling, 3BX filtering amplitude filtering and 3BX histogram smoothing.

Keeping all other aspects of the algorithm equal and only changing the histogram amplitude threshold has about the same effect as muting does. Figure 12 shows the output due to an amplitude threshold of 0.05 and Figure 13 shows the output due to an amplitude threshold of 0.15. Note that decreasing the histogram amplitude threshold (Figure 12) outputs our diffraction events as well as our dipping events and increasing the histogram amplitude threshold significantly decreases the output of our dipping events. In fact, increasing the histogram amplitude threshold to 0.2 effectively eliminates all events from our final migration except for our horizontal event.

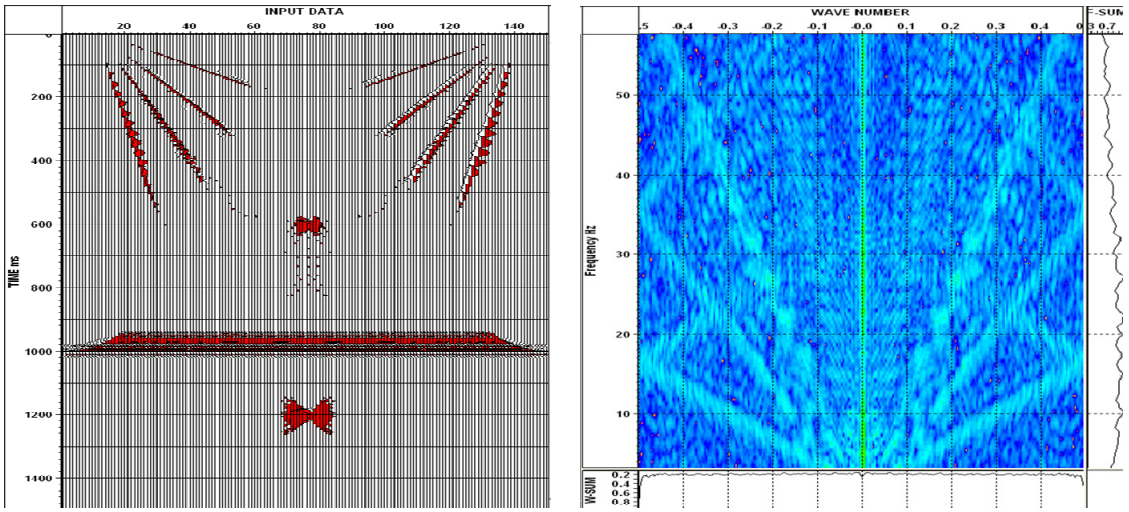

a) b)

FIG. 12 Migration and FK transform with a threshold of 0.05.

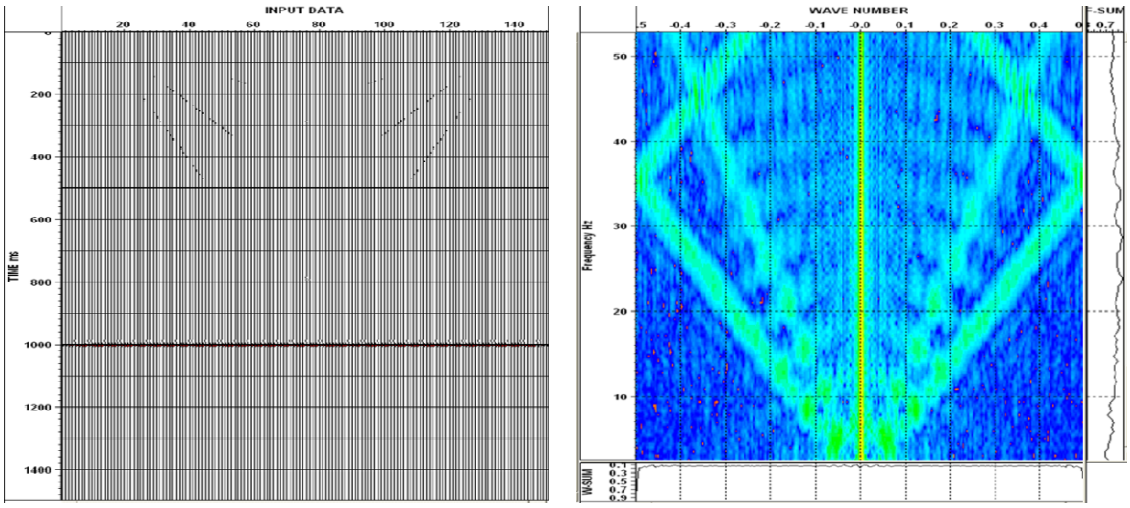

a) b)

FIG. 13 Migration and FK transform with a threshold of 0.15.

For interest's sake we also tried varying the histogram amplitude threshold based on the maximum amplitude within each diffraction spectrum, that is, the histogram was defined from the negative of the maximum of the absolute value to the positive of this value and divided into (for our case) 21 bins. Figure 14 shows the resulting output of a varying histogram method using the maximum amplitude of each diffraction – note that small amplitudes tend to be biased in this method and appear as the aliasing we see surrounding the middle diffraction event in Figure 14.

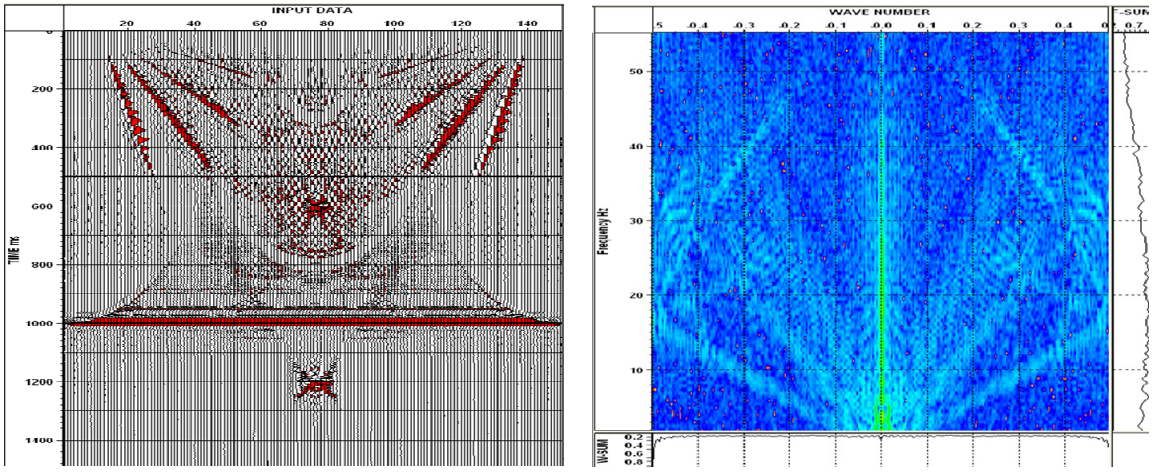

a) b)

FIG. 14 Migration and FK transform with a varying histogram amplitude based on the maximum amplitude within each diffraction amplitude.

CONCLUSIONS

A new method of anti-aliasing in Kirchhoff migration was explored which utilizes a histogram to isolate amplitude coherency along each diffraction shape. A histogram of amplitude frequencies is used to eliminate non-coherent and small amplitude data from the final migration summation. This method is data driven as opposed to model driven, which allows us to define a space varying migration aperture if desired without the need for a preconceived model.

We saw that this method produces a similar result to applying an energy threshold mute when the histogram is based on a constant amplitude scale. Varying the histogram amplitude to match the maximum amplitude for every diffraction has the result of biasing for small amplitude data which we want to eliminate. Another method to try in future work could be a histogram scale which varies according to time or depth.

We saw that this migration method works well for eliminating noise and spikes in the data while preserving dipping events, diffraction events, and flat events. This could have a practical application when examining spiky seismic data. There is a need to examine the effects of this method on different data sets while using different methods of varying the histogram scale and zeroing the histogram in order to understand its full potential.

FUTURE CONSIDERATIONS

There are many improvements that need to be made to make this concept practical. There are many other filtering methods that can be tried such as a median filter that can be very successful at removing spiked data.

In addition, the threshold parameters need to be time or depth varying to accommodate the changing size of the tangential area. Shallow data will require a smaller tangential area relative to a deep area. The size of the tangential area will also depend on the dip on the diffraction which could be related to the displacement from the center of the

diffraction. The width of non-tangential energy on the diffraction amplitude may also vary with dip and could also be related to the displacement from the center of the diffraction. An offset varying median filter may have better success.

The basic assumption only considered linear reflection energy. Curved surfaces and truncated events will also require consideration.

The data used was free from noise, and will have a significant effect on the choice of parameters.

This process will add considerable processing time to the migration. We assume that it would be used in special applications such as with data that has been acquires with considerable aliasing, or even significant noise. These applications will require significantly more development and testing.

ACKNOWLEDGEMENTS

The authors wish to thank the sponsors of the CREWES project for their support.

REFERENCES

Bancroft, J., 2008, A practical understanding of pre- and poststack migrations: University of Calgary Course Notes for GOPH 659.

Bancroft, J., 1993, Kirchhoff Migration FORTRAN Code

Gray, S.H., Etgen, J., Dellinger, J. Whitmore, D., 2001. Seismic migration problems and solutions, Geophysics, 66(5), 1622–1640

Kosloff et al., Migration Process Using a Model Based Aperture Technique, United States Patent Number 5629904, May 13 1997

Abma, R., Sun, J., and Bernitsas, N., 1999, Antialiasing methods in Kirchhoff migration: Geophysics 64, 1783-1792